07,18

Effect of graphene platelets pullout from ceramic matrix on the fracture toughness of ceramic/graphene composites

© S.V. Bobylev

[1] Institute of Problems of Mechanical Engineering, Russian Academy of Sciences, St. Petersburg, Russia
[2] Peter the Great Saint-Petersburg Polytechnic University, St. Petersburg, Russia

E-mail: bobylev.s@gmail.com

Received March 9, 2022
Revised March 9, 2022
Accepted March 13, 2022

A theoretical model is proposed that describes the effect of graphene platelets pullout on the fracture toughness of ceramic/graphene composites. The dependences of fracture toughness on the graphene concentration and the dimensions of graphene platelets are calculated using a yttria-stabilized zirconia (YSZ)/graphene composite as an example. Calculations predict that if graphene platelets pullout from ceramic matrix is the dominant mechanism, then the maximum fracture toughness is achieved in the case of the longest and thinnest possible graphene platelets, provided that the latter have sufficient strength and adhesion to the matrix. The model shows a good correlation with experimental data at low graphene concentrations.

Keywords: composites, graphene, ceramics, cracks, fracture toughness.

DOI: 10.21883/PSS.2022.06.53832.306

1. Introduction

Due to its excellent mechanical, optical and thermal properties, high electric conductivity and a high surface area, the graphene is a perfect filler for composites with polymer, metallic and ceramic matrices (see, for example, the reviews [1–3]). In particular, recently, various research teams have started a synthesis of ceramic nanocomposites containing nanoinclusions (of the thickness of several nanometers) of graphene or reduced graphene oxide [1–10]. The studies of these composites have shown that the graphene inclusions as platelets (hereinafter referred to as graphene nanoplatelets — GNPs) may lead to significant increase in fracture toughness, strength and electric conductivity of the ceramics [1–10]. In particular, small volume fractions of graphene or the reduced graphene oxide can lead to significant increase in ceramics crack growth resistance. For example, the paper [4] has found increase in the silicon nitride's fracture toughness by 135 percent after adding 1.5 volume percent of GNPs. Such sharp increase in the fracture toughness was attributed in [4], first of all, to formation of dense ensembles of the graphene sheets, which surround separate grains and cause a change in crack propagation direction. Li et al. [5] observed the increase in the fracture toughness of the aluminum oxide by 2.5 times after adding 2 vol.% of reduced graphene oxide. Another example of significant increase in the fracture toughness is tantalum carbide [6], wherein the GNPs increased the fracture toughness by 99 percent. At the same time, there are examples of ceramics strengthened by GNPs [3,7–10], which do not exhibit such strong strengthening. The structure studies have shown that increase in crack growth resistance of such nanocomposites is mainly due to crack bridging by the graphene inclusions, GNP pullout out of the matrix, as well as branching and curving of the cracks [4,6,8]. Hereinafter, „crack bridging" is understood as a mechanism of formation of links (bridges), which prevent crack banks from opening.

Previously, some authors [11–13] had theorized the strengthening effects correlated to GNPs, in composites with a ceramic and polymer matrix. In particular, Zhang et al. [11] evaluated contribution of the graphene platelets pullout to the fracture toughness of a polymer strengthened by GNPs. For that, they calculated the work required to pullout GNPs out of the matrix near a crack tip. However, their model seems to be simplified, since they assumed that each GNP would fully pull out immediately after the crack front passes past the platelet, which can be true only for very short platelets. Moreover, they neglected the bridging contribution in an area behind the crack tip. Ramirez and Osendi [12] applied a solution [14], found for ceramics strengthened by fibers, for ceramics strengthened by GNPs, which did not take into account a real flat shape of the GNP, yet. Both the studies [11,12] have obtained a linear dependence between a critical energy release rate and a volume fraction of graphene.

Chou and Green [15] and Ovid'ko and Sheinerman [13] calculated a deflection effect (deviation from straight-line propagation) of cracks in the ceramics strengthened by silicon carbide and GNPs, respectively. They demonstrated that even with a small volume fraction of graphene (up to 2−4%) the crack deflection can increase the crack resistance by several dozens percent. At the same time,

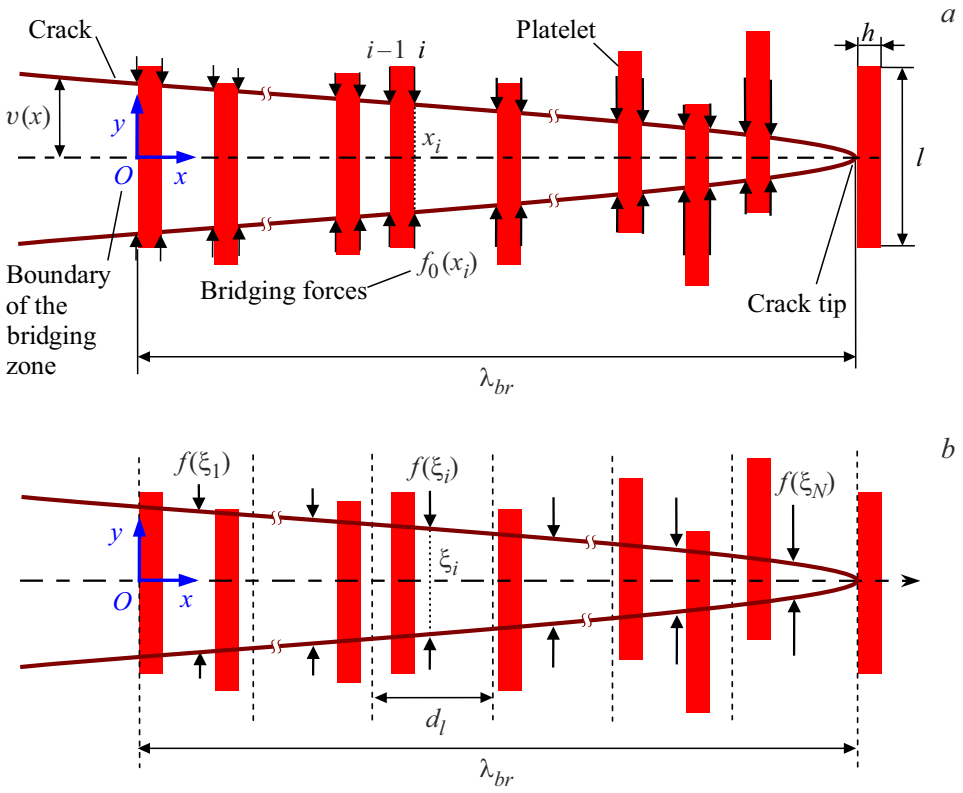

Figure 1. *a* — a crack in the ceramics/graphene composite. In the bridging zone, forces preventing crack opening are presented as a discrete system of point forces $f_0(x_i)$. *b* — an illustration of the calculation diagram. The bridging zone is divided into layers of the same width d_i, each has an integral force $f(\xi_i)$ acting.

electron microscopy observation of the cracks and fracture surfaces of the ceramics/graphene composites (see, for example, reviews [2,3]) underline a very important role of crack bridging in combination with GNP pullout for increasing the crack resistance of such composites. An important role of bridging is additionally confirmed by a nature of crack growth resistance dependences [3] (which show significant increase in the fracture toughness when a crack length is increasing), observations of „wrinkling" of GNPs [2,3] and GNP wrapping about the grains [4,16], which can strongly increase a friction force between the GNP and the ceramic matrix during pullout.

The present paper proposes a theoretical model, which describes the GNP pullout process out of the ceramic matrix and its influence on the fracture toughness of the material. The model is developed from a previously proposed model of Bobylev and Sheinerman [17], which, in turn, uses a method originally developed by Shao et al. [18] to describe the crack growth resistance of nacre. Differences of the present model from the previous one [17] are described in the next section.

2. Theoretical model

Let us consider propagation of the crack in the GNP-strengthened composite sample. For this, we consider a model straight semi-infinite mode I crack, which crosses the system of identical platelets (of the same length l, width h and thickness w) perpendicular to a crack plane (Fig. 1). In area to the left of the crack tip, where the distance between the crack surfaces is less than the GNP length (hereinafter to be called a bridging zone), the platelets form links between the crack surfaces. The friction between the GNP and the ceramic matrix creates forces preventing the crack opening, thereby increasing the fracture toughness of the material.

Previously, the paper [17] considered the configuration of GNPs located symmetrically in relation to a crack plane, i.e. centers of all the GNPs were exactly in the crack plane along one line. Such configuration is artificial and leads to overestimation of the pullout effect, as at this the pullout resistance forces are maximum ones for each platelet. The present model assumes that the platelets are located randomly in relation to the crack plane (but still perpendicular to it). In case of random arrangement of the platelets in relation to the crack plane, the friction forces are different at upper and lower crack banks. However, the process of pullout of the platelet out of the matrix is controlled by a lesser force (at that side of less immersion into the matrix). It is obvious that the initial depth of immersion may vary from 0 to $l/2$, whereas in the model [17] it is exactly equal to $l/2$. In order to take into account the random distribution of GNPs in relation

to the crack plane, we assume that the initial depth of GNP immersion into the matrix is equal to the averaged immersion depth, i.e. $l/4$. Then, in a Cartesian coordinate system (x, y), with the origin at the bridging zone boundary (Fig. 1) the friction forces at the graphene/ceramics interface boundaries (per a unit length in the direction perpendicular to the plane of Fig. 1) are written down as per the study [17] as follows:

$$f_0(x_i) = \tau(x_i)\left[\frac{l}{4} - v(x_i)\right]. \quad (1)$$

Here, x_i — the coordinates of the matrix/platelet interface boundaries, along which the forces are acting (i assumes the values from 1 to a number equal to the total number of the interface boundaries), $v(x_i)$ — the value of crack opening at the point $x = x_i$ (which is equal to a GNP pullout length at the same place), $\tau(x_i)$ is the average friction stress at the interface boundary between the graphene and matrix. Further on, for the case under study of the ceramics/graphene composites, we assume that the stress $\tau(x_i)$ does not depend on the crack opening value in the point and think that $\tau(x_i) = \tau_0$, where τ_0 — the material constant.

It should be noted that in the general case the GNPs are not laid parallel to each other. However, there are synthesis procedures, which provide structures to be sufficiently close to our model. Thus, in the ceramics/graphene composites produced by the spark plasma sintering and under action of a uniaxial compression, the GNPs usually tend to be predominantly laid in planes, which are normal or almost perpendicular to the compression direction [2,3]. For example, in the Si_3N_4/graphene composites produced as per the paper [19] by this method, more than 80% of the GNPs were oriented within $\pm 15^\circ$ from the predominant direction of orientation. That is why in the present study we consider the case of the ceramics/graphene composites with the parallel GNPs, which are subjected to a single-axis tensile load applied along the platelets. Consequently, we consider the crack plane to be strictly perpendicular to the GNPs.

As the GNPs are randomly distributed in the material, we do not know their coordinates and, therefore, can not directly determine the forces f_0. Nevertheless, we can describe the forces impeding the crack opening by applying the following procedure from the paper [17]. Let us divide the crack bridging zone into N identical layers, whose width d_l along a crack growth direction is small in comparison with the length λ_{br} of the bridging area (see Fig. 1, *b*). In this case, the crack opening v can be considered as a constant within each layer. Let us replace the ensemble of all concentrated forces acting within each layer at the matrix/platelet interface boundaries (whose coordinates are not known to us) by a single coordinated force $F(\xi_i)$, which is defined a sum of forces created by all GNPs within this layer. For definiteness, we put these forces into the centers of each of the layers specified by the coordinates (in the coordinate system shown in the Fig. 1):

$$\xi_i = (i - 1/2)d_l, \quad i = 1, 2, \ldots, N. \quad (2)$$

The $F(\xi_i)$ forces can be specified as:

$$F(\xi_i) = 2\tau_0[l/4 - v(\xi_i)]wN_{gr}. \quad (3)$$

Here, $2\tau_0[l/4 - v(\xi_i)]$ is a double force (to take into account friction at both side surfaces of the GNPs), being specified by the formula (1), w — the GNP width (along the direction perpendicular to the plane of Fig. 1) and N_{gr} — the averaged number of GNPs within one layer. We think that GNPs are uniformly distributed within the bulk of the materials, so, taking into account the identical width of all the layers, the value N_{gr} is also the same for any layer. The number N_{gr} can be evaluated in the following way. If the crack width is designated (in a direction perpendicular to the plane of Fig. 1) as W, then all the GNPs, which can intersect the crack plane, stay within a parallelepiped with dimensions $2l \times d_l \times W$ and, consequently, a volume $V = 2ld_lW$. Total volume of the graphene V_{gr} within this parallelepiped is equal to $V_{gr} = N_{gr}V_0 = N_{gr}lwh$ (here $V_0 = lwh$ — a volume of a single GNP). The volume fraction c of graphene in the material by the definition is: $c = V_{gr}/V = N_{gr}wh/(2d_lW)$. From here we find that:

$$N_{gr} = \frac{2cd_lW}{wh}. \quad (4)$$

From (3) and (4) we find the force $F(\xi_i)$ as:

$$F(\xi_i) = \frac{cd_lW}{h}\tau_0[l - 4v(\xi_i)]. \quad (5)$$

In turn, the force per the unit length of the layer along the direction of the axis z (see Fig. 1, *b*) is specified as:

$$f(\xi_i) = F(\xi_i)/W = \frac{cd_l}{h}\tau_0[l - 4v(\xi_i)]. \quad (6)$$

Note that the forces $f(\xi_i)$ do not depend on the w size (width) of GNP.

Within the approach of the papers [17,18], the fracture toughness K_{IC} of the composite is written down as:

$$K_{IC} = K_I^0 - K_I^{br}, \quad (7)$$

where K_I^0 is the fracture toughness without taking into account the bridging effect, and K_I^{br} — the stress intensity coefficient created by the friction forces during GNP pullout. The value is negative and specified by the following expression [17,18]:

$$K_I^{br} = -\sqrt{\frac{1}{2\pi}}\frac{cd_l\tau_0}{h}\sum_{i=1}^{N}\frac{l - 4v(\xi_i)}{\sqrt{\lambda_{br} - \xi_i}}. \quad (8)$$

The absolute value of the magnitude K_I^{br} is increasing with increase in λ_{br}, to ultimately get to saturation. At this, the crack is coming to the steady-state mode of growth [18],

wherein it is growing, but the bridging area keeps its size constant. In the steady-state mode, a new bridge forming at the right end of the bridging area is always accompanied by full GNP pullout at the left end.

In order to use the formula (8), it is necessary to know the values $v(\xi_i)$ of the crack opening. They are found by solving the following system of the N linear equations [18]:

$$v(\xi_i) = \frac{4K_I^0\sqrt{\lambda_{br}-\xi_i}}{\sqrt{2\pi}E} + \frac{2cd_l\tau_0\sqrt{\lambda_{br}-\xi_i}}{\pi Eh}\sum_{n=1}^{N}\frac{l-4v(\xi_n)}{\sqrt{\lambda_{br}-\xi_n}}$$

$$-\frac{cd_l\tau_0}{\pi Eh}\,p.v.\sum_{n=1}^{N}[l-4v(\xi_n)]\ln\frac{\sqrt{\lambda_{br}-\xi_i}+\sqrt{\lambda_{br}-\xi_n}}{|\sqrt{\lambda_{br}-\xi_i}-\sqrt{\lambda_{br}-\xi_n}|}. \quad (9)$$

Here, E — the Young modulus of the matrix, and $p.v.$ means a Cauchy principal value (a definition and instructions to calculate this value can be found in the Appendix to the article [18]).

3. Results and discussion

In this section we calculated dependences of the fracture toughness of the ceramics/graphene composites on different parameters in the examplary case of yttria-stabilized zirconia (YSZ)/graphene composite, using the experimental data from the paper [10]. All the calculations were carried out for the steady-state mode of crack propagation, which is characterized by quite large lengths of the cracks (see the previous section). The model is calibrated using the experimental data [10] for the case of the low content of graphene, when nobody expects decrease in the fracture toughness due to increase in porosity, as it is typical for the ceramics/graphene composites with a high concentration of graphene. The calibration means selecting a value of the parameter τ_0, at which there is good coincidence with the experimental data. The paper [10] has produced samples of the YSZ/graphene composite with the GNP average thickness $h = 7$ nm. The GNP average length is not specified, but structure microphotographs show that the typical GNP length is about several hundred nanometers (the most probable is within the range of 300−500 nm). The tests as per the paper [10] have shown that $K_I^0 = 7.8\,\text{MPa}\cdot\text{m}^{1/2}$, the crack resistance increase coefficient $\eta = K_{IC}/K_I^0 \approx 1.038$ and 1.09 for $c = 0.25$ and 0.5 vol.%, respectively.

For the value of the Young module $E = 577$ GPa [20], $h = 7$ nm and $l = 500$ nm, good coincidence with the experimental data of the paper [10] is achieved at the value $\tau_0 = 370$ MPa. Our calculations give out $\eta \approx 1.04$ at $c = 0.25$ vol.% and $\eta \approx 1.08$ at $c = 0.5$ vol.%. At the higher values of the graphene concentration, the experimental data of the paper [10] diverge from our calculations. For example, at $c = 2$ vol.% our model gives out $\eta \approx 1.27$, whereas the measured increase in the fracture toughness is $\sim 64\%$.

Thus, the value $\tau_0 = 370$ MPa provides fairly good coincidence with the experimental data at the lower graphene concentrations. We compared it with available data obtained by the modeling, for different ceramics/graphene systems (unfortunately, for the YSZ/graphene system we could not find data of experiments or modeling). For example, for the Al_2O_3/graphene system, the value of $\tau_0 = 395.77$ MPa was found [21]. Thus, our evaluation obtained is quite realistic. It should be noted that the model of the paper [17] used $\tau_0 = 200$ MPa, which is attributed to the above-mentioned overestimation of the pullout effect due to symmetrical GNP arrangement.

Now, we can calculate the dependences of the crack resistance increase coefficient η on different parameters (c, l, h) in order to obtain theoretical evaluations of the strengthening due to the crack bridging. The curves were plotted for $\tau_0 = 370$ MPa, $E = 577$ GPa [20] and $K_I^0 = 7.8\,\text{MPa}\cdot\text{m}^{1/2}$ [10]. The Fig. 2, *a* shows the dependences of the strengthening degree on the volume fraction of graphene c for various values of the GNP l, calculated for $h = 7$ nm. The Fig. 2, *a* shows that the η is growing with increase in the content c of graphene in the composite, while the normalized increase in the fracture toughness $(K_{IC}-K_I^0)/K_I^0 = \eta-1$ is growing with the volume fraction of graphene approximately as $\eta-1 \sim c^{0.8}$. It means that our model predicts a faster growth of crack resistance in comparison with the previous models [11,12], which predicted $K_{IC}-K_I^0 \sim c^{1/2}$.

The Fig. 2, *b* shows the dependences of the coefficient η on the GNP length l for various values of the thickness h, calculated at $c = 1$ vol.%. The Fig. 2, *b* shows that the fracture toughness is growing with increase in the GNP length. Despite that for the fixed volume fraction of graphene the bigger length of the platelet, the less the number of the platelets in the composite, it is much more difficult to pull out the longer GNP out of the matrix due to a bigger area of the interface boundary, thus securing increase in the fracture toughness. The dependences in the Fig. 2, *b* are true for platelet lengths below the values, at which the platelets of graphene can be broken. The critical length of the fracture of the graphene platelets can be evaluated from the equation $\tau_0 l_c = \sigma_m h$, where σ_m — the GNP tensile strength. The last relationship gives out: $l_c/h = \sigma_m/\tau_0$. If evaluating the strength of graphene tensile platelets by the strength of the monolayer graphene (from 35 GPa for some samples of polycrystalline graphene up to 130 GPa for pure graphene [22]), then we obtain: $l_c/h = 175-650$. It means that all the curves of the Fig. 2, *b* are laid in one area, in which there is no GNP fracture for certain.

The Fig. 2, *c* shows the dependences of the coefficient η on the GNP thickness h for different values of the length l, calculated at $c = 1$ vol.%. The Fig. 2, *c* shows that the crack growth resistance quickly drops with increase in the GNP thickness. This is due to the fact that the more the GNP thickness, the less their number in the composite (with the fixed volume fraction of graphene), so the less the number of bridges connecting the banks of the cracks. That is, at the specified volume fraction of graphene the finer GNPs

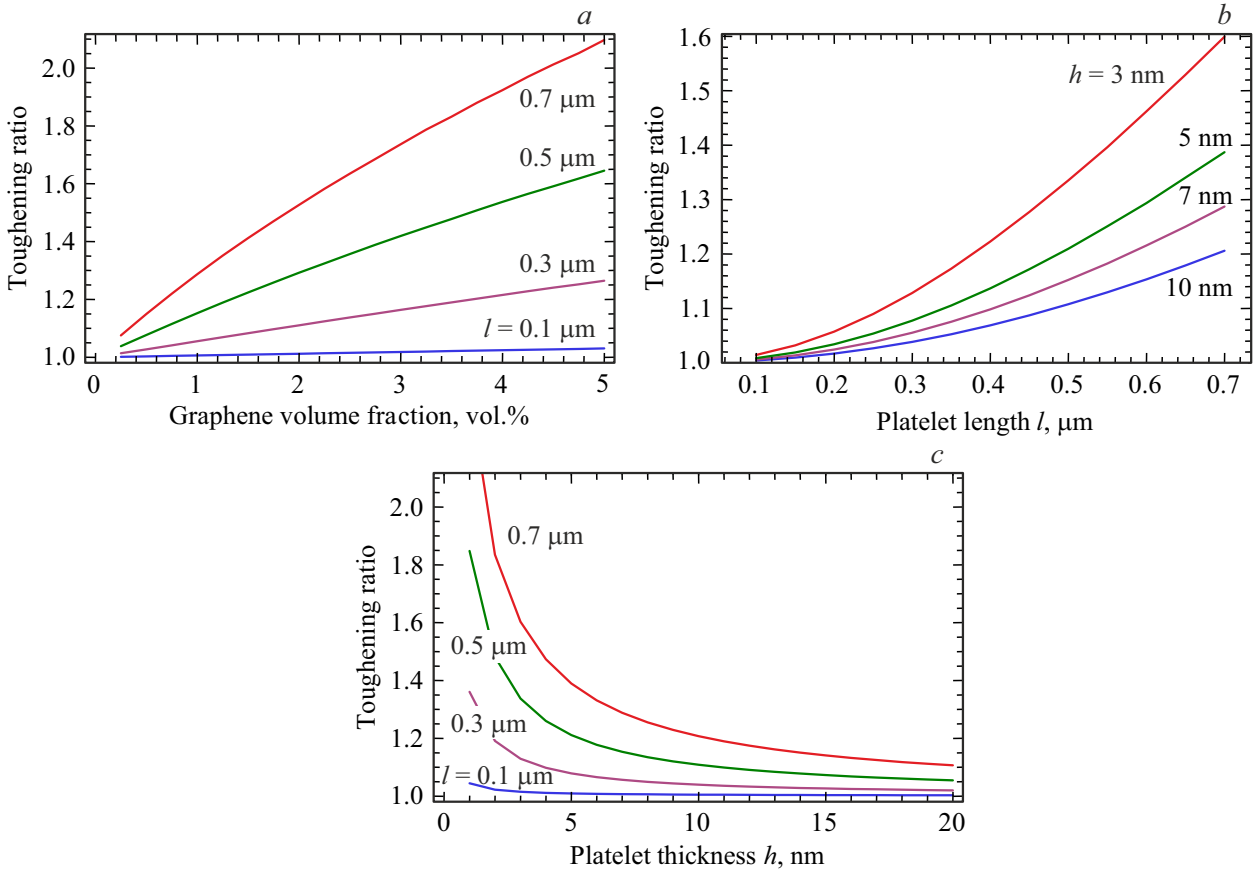

Figure 2. Dependences of the crack resistance increase coefficient of the YSZ/graphene composite on: (*a*) a volume fraction of graphene for the thickness of the graphene platelets $h = 7$ nm and different values of the length l; (*b*) a length of the graphene platelets for the volume fraction of graphene $c = 1\%$ and different values of the thickness h; (*c*) a thickness of the graphene platelets for the volume fraction of graphene $c = 1\%$ and different values of the length l.

provide for the higher fracture toughness. However, the simple change of the GNP thickness without changing a number thereof does not affect the crack growth resistance.

As a whole, Fig. 2 shows that if GNP pullout is a dominating mechanism to control propagation of the cracks in the ceramics/graphene composites, the fracture toughness can increase by up to $\sim 100\%$ depending on the concentration of graphene in the composite and the GNP sizes. This figure is comparable to a typical, experimentally observed growth of the crack resistance [9,10,22] (usually about 20–60%).

4. Conclusion

Thus, we have proposed a model describing an impact of matrix GNP pullout on the crack growth resistance of the ceramics/graphene composites. The model was taken to consider a mode I crack propagating perpendicular to the parallel systems of GNPs, whose pullout out of the ceramic matrix behind the crack tip impedes the crack opening. Based on the YSZ/graphene composite, we showed that increase in the fracture toughness $K_{IC}-K_I^0$ depends on the volume concentration c of graphene approximately as $K_{IC}-K_I^0 \sim c^{0.8}$. The calculations also showed that for the specified concentration of graphene longer and thinner GNPs provided the higher crack growth resistance.

Funding

This study was financially supported by the Russian Science Foundation (grant No. 18-19-00255).

Conflict of interest

The author declares that he has no conflict of interest.

References

[1] I.A. Ovid'ko. Rev. Adv. Mater. Sci. **34**, *1*, 19 (2013).
[2] H. Porwal, S. Gresso, M.J. Reece. Adv. Appl. Ceram. **112**, *8*, 443 (2013).
[3] A. Centeno, V.G. Rocha, B. Alonso, A. Fernandez, C.F. Gutierres-Gonzalez, R. Torrecillas, A. Zurutuza. J. Eur. Ceram. Soc. **33**, *15–16*, 3201 (2013).

[4] L.S. Walker, V.R. Marroto, M.A. Rafiee, N. Koratkar, E.L. Corral. ACS Nano **5**, *4*, 3182 (2011).
[5] B. Lee, M.Y. Koo, S.H. Jin, K.T. Kim, S.H. Hong. Carbon **78**, 212 (2014).
[6] A. Nieto, D. Lahiri, A. Agarwal. Mater. Sci. Eng. A **582**, 338 (2013).
[7] J. Lui, H. Yan, K. Jiang. Ceram. Int. **39**, *6*, 6215 (2013).
[8] H. Porwal, P. Tatarko, S. Grasso, J. Khaliq, I. Dlouhý, M.J. Reece. Carbon **64**, 359 (2013).
[9] J.H. Shin, S.H. Hong. J. Eur. Ceram. Soc. **34**, *5*, 1297 (2014).
[10] J. Liu, H. Guo, Y. Su, L. Wang, L. Wei, G. Yang, Y. Yang, K. Jiang. Mater. Sci. Eng. A **688**, 70 (2017).
[11] L. Zhang, X.G. Zhang, Y. Chen, J.N. Su, W.W. Liu, T.H. Zhang, Y.T. Wang. Appl. Phys. Lett. **105**, *16*, 161908 (2014).
[12] C. Ramirez, M.I. Osendi. Ceram. Int. **40**, *7*, 11187 (2014).
[13] I.A. Ovid'ko, A.G. Sheinerman. Rev. Adv. Mater. Sci. **43**, *1/2*, 52 (2015).
[14] G.H. Campbell, M. Rühle, B.J. Dalgleish, A.G. Evans. J. Am. Ceram. Soc. **73**, *3*, 521 (1990).
[15] Y.S. Chou, D.J. Green. J. Am. Ceram. Soc. **76**, *8*, 1985 (1993).
[16] I. Ahmad, M. Islam, H.S. Abdo, T. Subhani, K.A. Khalil, A.A. Almajid, B. Yazdani, Y. Zhu. Mater. Des. **88**, 1234 (2015).
[17] S.V. Bobylev, A.G. Sheinerman. Rev. Adv. Mater. Sci. **57**, *1*, 54 (2018).
[18] Y. Shao, H.-P. Zhao, X.-Q. Feng, H. Gao. J. Mech. Phys. Solids **60**, *8*, 1400 (2012).
[19] O. Tapasztó, L. Tapasztó, H. Lemmel, V. Puchy, J. Dusza, C. Balázsi, K. Balázsi. Ceram. Int. **42**, *1*, 1002 (2016).
[20] I.D. Muhammad, M. Awang, O. Mamat. Adv. Mater. Res. **845**, 387 (2014).
[21] X. Wang, J. Zhao, E. Cui, X. Tian, Z. Sun. Nanomaterials **11**, *6*, 1374 (2021).
[22] P.Y. Huang, C.S. Ruiz-Vargas, A.M. van der Zande, W.S. Whitney, M.P. Levendorf, J.W. Kevek, S. Garg, J.S. Alden, C.J. Hustedt, Y. Zhu, J. Park, P.L. McEuen, D.A. Múller. Nature **469**, 389 (2011).